JOURNAL OF EXPERIMENTAL AND THEORETICAL PHYSICS, 2024, Vol. 166, No. 3 (9), pp. 374–385

ELECTRONIC PROPERTIES OF SOLID

INFLUENCE OF MAGNETIC FIELD ON CONDUCTIVITY OF SUPERCONDUCTOR—INSULATOR — NORMAL METAL TUNNEL STRUCTURE

© 2024 A. B. Ermakov[a], M. A. Tarasov[a], V. S. Edelman[b*]

[a] Kotelnikov Institute of Radio Engineering and Electronics, Russian Academy of Sciences, 125009, Moscow, Russia
[b] Kapitza Institute for Physical Problems, Russian Academy of Sciences, 119334, Moscow, Russia

*e-mail: edelman@kapitza.ras.ru

Received October 27, 2023
Revised March 01, 2024
Accepted April 25, 2024

Abstract.The results of experiments on the effect of a magnetic field on the conductivity of superconductor — insulator — normal metal tunnel structures are analyzed at temperatures much lower than the critical temperature of the superconductor Tc and at low voltages at which the single-electron current Isingle is comparable to or less than the sub-gap Andreev current IA= In+Is. These two components of the Andreev current are associated with the diffusive motion of correlated pairs of electronic excitations in the normal and, accordingly, superconducting layers of the structure. With the orientation of the field perpendicular to the structure with lateral dimensions greater than the penetration depth, the transition from an inhomogeneous field distribution to a vortex structure is traced. At field orientations both in the plane of the structure and perpendicular to it, the single-electron current increases due to the influence of the field on the superconducting gap Δc. The conductivity due to the Andreev current In =kntanh(eV/2kTeff) decreases due to an increase in the effective temperature Teff. The decrease in the Is contribution is associated with a decrease of the gap. We do not know of any works that consider the influence of the magnetic field on this component of the tunneling current. It is shown that at low voltages, the so-called Dynes current, due to an imaginary addition to the gap energy due to the influence of defects in the superconductor, does not contribute to the conductivity of the tunnel structure.

Keywords: *superconductivity, tunnel structure, low temperatures, magnetic field, andreev current*

DOI: 10.31857/S004445102409e098.

1. INTRODUCTION

Despite numerous studies on the conductivity of thin-film superconductor-insulator-normal metal (SIN) microstructures at low temperatures, questions remain regarding the influence of a permanent magnetic field. While there are many theoretical works on this topic, experimental studies are quite limited. Among known publications, papers [1–3] can be mentioned, which traced the pair-breaking effect in the superconducting electrode of SIN under magnetic field, leading to a decrease in the energy gap and increase in tunnel current at bias V, close to voltage $V_c = \mathsf{D}_c / e$, where D_c is the gap in the superconductor spectrum. In particular, [3] investigated this effect for aluminum-insulator-copper structure. The creation of Abrikosov vortices in aluminum films in normal field was observed in [4, 5]. The suppression of anomalous differential conductivity at $V = 0$ by magnetic field applied in the structure plane is shown in [6,7]. However, there are no works where all these phenomena, as well as the field's influence on other subgap current components, were observed on a single sample and at different magnetic field orientations. The aim of the proposed work is to describe and analyze experiments meeting this requirement. We limit ourselves to the region of

small bias $V \leq 0.5V_c$, where thermal effects - heating or electronic cooling, which greatly complicate the analysis of results, have practically no effect on the tunnel current.

The SIN current consists of single-electron current and subgap current. The single-electron current is due to tunneling of thermally excited electrons above the Fermi level from normal metal to free states above the superconductor gap with energy conservation (for opposite bias, tunneling of superconductor excitations to free states below the Fermi level). At electronic temperature $T_e << T_c$ and $V \leq 0{,}7V_c$ it is described with accuracy of about 1 percent by formula [8]

$$I_{single} = \frac{1}{eR_n}\sqrt{2\pi kT_e\Delta_c}\exp\left[-\frac{\Delta_c}{kT_e}\right]\frac{eV}{kT_e}. \quad (1)$$

At $V \leq V_\Delta / 2$ and temperature $T \leq 0.2T_c$ (T_c — critical temperature of superconductivity) this current becomes small and the main contribution comes from subgap Andreev current and Dynes current. Andreev conductance is much lower than SIN conductance in normal state of superconductor, but remains at noticeable level in “dirty” metals, when electron pairs diffuse over large distances maintaining coherence, and in thin films repeatedly return to the boundary between metals, which increases their tunneling probability. This current component is described by formula proposed in [9]:

$$I_{Andreev} = I_n \quad I_s = \frac{\hbar}{e^2R_n^2S\nu_n d_n}\text{th}\frac{eV}{2kT_e} +$$

$$+\frac{\hbar}{e^2R_n^2S\nu_s d_s}\frac{eV/\sqrt{1-eV/\Delta_c}}{2\pi\Delta_c}. \quad (2)$$

Currents I_n and I_s correspond to pair diffusion in the bulk of normal metal and superconductor respectively, R_n is the junction resistance in normal state, S is its area, d_n, d_s are layer thicknesses, and ν_n, ν_s are density of states. Although all quantities in this formula are either known or can be measured, the measured currents usually differ significantly from theoretical values. The main reason is considered to be the inhomogeneity of the barrier layer, due to which its transparency for single-electron tunneling is higher than for two-electron tunneling. Based on this, in [7] it was proposed for description of experimental results to use formula

$$I_{Andreev} = I_n + I_s =$$

$$= k_n h\frac{eV}{2kT_{eff}} + k_s\frac{eV/\sqrt{1-eV/\Delta_c}}{\Delta_c}, \quad (3)$$

where parameters k_n, k_s and T_{eff} are determined by fitting experimental I-V characteristic. Paper [9] is not the only one calculating Andreev current. For instance, in [10] a similar result was obtained but with certain differences. And these are not only different numerical coefficients, but different dependence of current on bias voltage:

$$I_{Andreev} = I_n + I_s =$$

$$= \frac{3\pi\hbar}{2e^2R_n^2S\nu_n d_n}\text{th}\frac{eV}{2kT_e} +$$

$$+\frac{2\hbar}{e^2R_n^2S\nu_s d_s}\frac{eV/\sqrt{1-(eV/\Delta_c}}{\Delta_c}. \quad (4)$$

In this case, in the expression for current I_s under the square root there is bias voltage not in first power as in (2), but squared. In the first case, differential conductance dI/dV at low voltages increases linearly, while in the second case it is practically constant. Functionally, according to (4), this contribution to current coincides with Dynes current, which in most known works is considered responsible for excess current. This is single-electron subgap current, due at $T << T_c$ to broadening of superconductor excitation spectrum because of defects. Based on experimental data, it is shown that spectrum takes form [11]

$$\rho(E,\gamma) = \frac{E - i\gamma}{\sqrt{(E - i\gamma)^2 - \Delta_c^2}},$$

where $\gamma << \Delta_c$ is empirical parameter describing this broadening. Based on this spectrum, expression for current is obtained (for example, [12]

$$I_{Dynes} = \frac{\gamma}{\Delta_c}\frac{V/\sqrt{1-(eV/\Delta_c)^2}}{R_n}. \quad (5)$$

In this work, a more detailed than in [7] analysis of experiments on SIN conductance study at cooling to temperature about 0.1 K in magnetic field up to 30 mT is conducted. In field normal to SIN

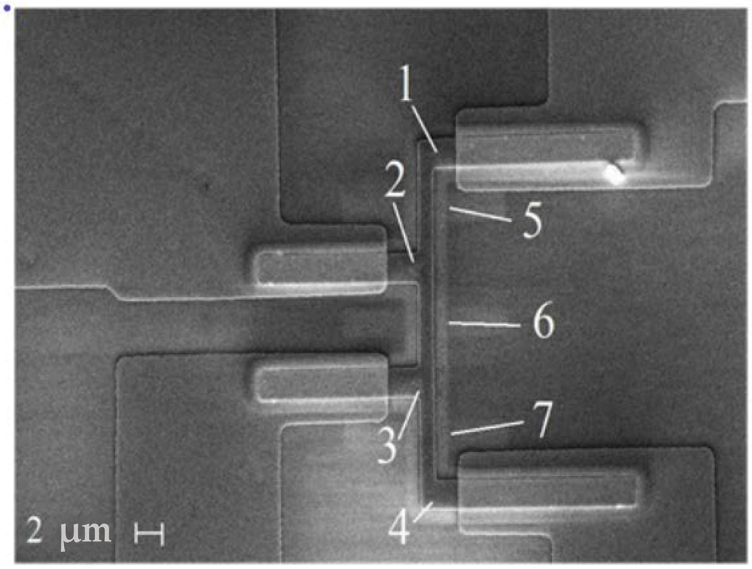

Fig. 1. Scanning electron microscope image of SINIS structures. 1, 2, 3, 4 — tunnel junctions, 5, 6, 7 — suspended normal bridges

surface, in structure with lateral dimensions much larger than penetration depth into superconductor, transition from inhomogeneous field distribution to structure of Abrikosov vortices was traced. This allowed estimating l and correlation length x . In [7] mainly influence of field only on Andreev current component I_n. was considered. Here, based on results of work [3], effect of uniform field lying in SIN plane with superconducting film thickness $d < l$, on single-electron conductance was studied. It was established that pair breaking leads to faster than found in [3] quadratic decrease of parameter D_c, while formula (1) still describes single-electron current. It is shown that at $G_{single} \leq 0.2G_N$ (G_N —normal conductance) transition occurs from Dynes current (5) to current exponentially decreasing with voltage reduction. Knowledge of single-electron current allowed reliable determination of Andreev current components $I_n$and I_s. Results related to current I_n, practically coincide with those obtained in [7]. Current I_s depends on field more weakly than I_n. This dependence can be described as due to quadratic decrease of gap with field. Qualitative explanation is given for changes in current components at normal field with its inhomogeneous distribution.

2. EXPERIMENTAL TECHNIQUE

Most of the experiments were conducted with test structures described in work [7]. Figure 1 shows an image of such a structure. It contains 4 copper-aluminum tunnel junctions (1–4) connected by a copper strip deposited on the oxidized surface of aluminum, which was directly deposited on a silicon substrate. In regions 5–7, the aluminum beneath the copper has been etched away. The film thicknesses are 20 nm (copper) and 80 nm (aluminum), the areas of SIN1 and SIN2 are 8 and 10 μm respectively. On a chip with 16 contact pads along the edges, there are 4 such structures. 20 SINs were tested on two chips. The results obtained for them are close to each other. To avoid overloading the presentation, most of the results below are given for one of the SIN1s, which has the most pronounced Andreev current.

Current-voltage characteristics were measured using DC four-probe method. To protect tunnel junctions from parasitic radiation, 0.8 MOhm resistors cooled to 0.4 K were included in the supply wire circuit. The structure topology allowed measuring both SINIS junction characteristics, for example, by passing current through junctions 1 and 4 and measuring voltage across them, and single SIN characteristics, for example, by measuring voltage at contacts and current through contacts 1–4. An automated data acquisition system based on a portable laptop computer and NI USB DAC-ADC unit was used. Current I was set by a 16-bit DAC. The voltage V amplified by a low-noise amplifier was converted by a 16-bit ADC. Differential conductance $G(V) = dI / dV$ or differential resistance R_d were determined by numerical differentiation of

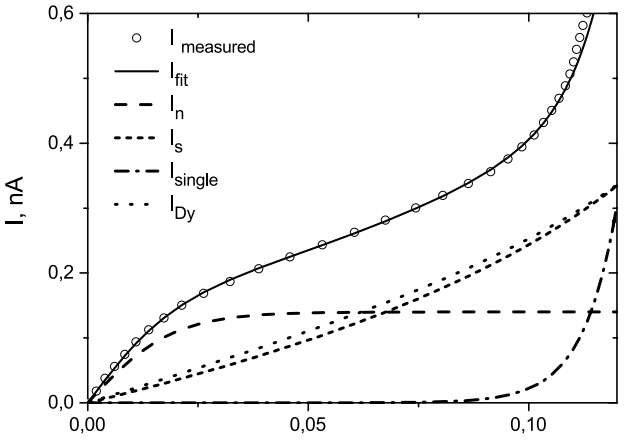

Fig. 2. Measured current-voltage characteristic of SIN and its fitting with theoretical models. The fitting uses values Δ_c/k = 2.18 K and R_n = 29 Ohm, determined from the temperature dependence of tunnel current, and values k_n = 0.135 nA, k_s = 0.32 nA or $\gamma/\Delta = 6.2\cdot10^{-5}$, T_{eff} = 0.11 K and T_e = 0.094 K. Electronic temperature is estimated from single-electron current at chip temperature $T \simeq 0.09$ K. Usually T_e is slightly higher than T due to radiation penetration from the environment

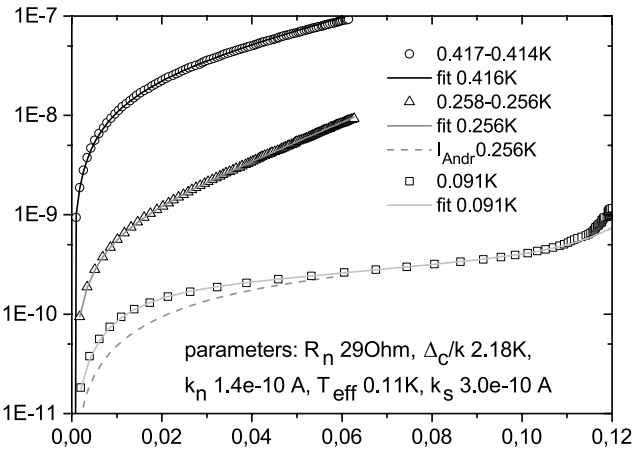

Fig. 3. Determination of parameters Δ_c and R_n from I-V characteristics measured at different temperatures, considering small correction for Andreev current. Andreev current parameters were established at T = 0.09 K

current-voltage characteristics. Measurements were conducted using a computer-controlled insert dilution refrigerator [13], where samples are placed inside a screen with temperature 0.4–0.5 K at the top of the device on a cooled holder. Samples were installed horizontally or vertically. Vertically directed magnetic field, created by a solenoid located outside the cryostat, is applied approximately normal or tangential to the tunnel junction plane with an error of several degrees. To change the field direction, the solenoid can be tilted within $\pm\ 10^0$.

3. EXPERIMENTAL RESULTS

Fig. 2 and 3 show the measured I-V characteristics without magnetic field for this structure and their fitting at chip temperature T_{chip} = 0.09 K and current components (Fig. 2), and at several temperatures, Fig. 3. This allowed determining the initial values of all parameters: Δ_c, R_N, k_n, k_s (for Andreev current according to [9]) or γ (for Dynes current), T_{eff} and electronic temperature T_e, which is slightly higher than T_{chip} due to heating by parasitic radiation penetrating from the room. It was impossible to directly measure the small resistance R_N and determine Δ_c by the position of conductance maximum at $V \simeq V_c$ as it is in series with the resistance of current-feeding tracks of approximately the same magnitude. Because of this, the maximum in experimental dependencies of differential conductance on voltage did not

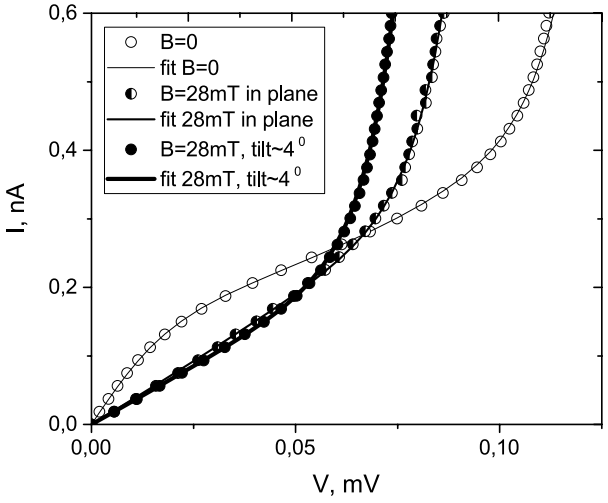

Fig. 4. I-V characteristics under the influence of magnetic field applied in the structure plane and at an angle of approximately 4° to it

manifest at all even in the absence of magnetic field. It could only be revealed after estimating the resistance of current leads, based on the calculated value of and introducing a correction for voltage drop.

Figure 4 shows CVC measured in zero field and in a field of 28 mT, and their fitting using equations (1) and (3). In an inclined magnetic field, it affects the current change more strongly than when applied in-plane. This is what makes it possible, by tilting the solenoid, to achieve field alignment relative to the SIN plane with accuracy of the order of 1^o. As can be seen, the used functional dependencies well describe the experimental results, which confirms the absence of thermal effects during current flow

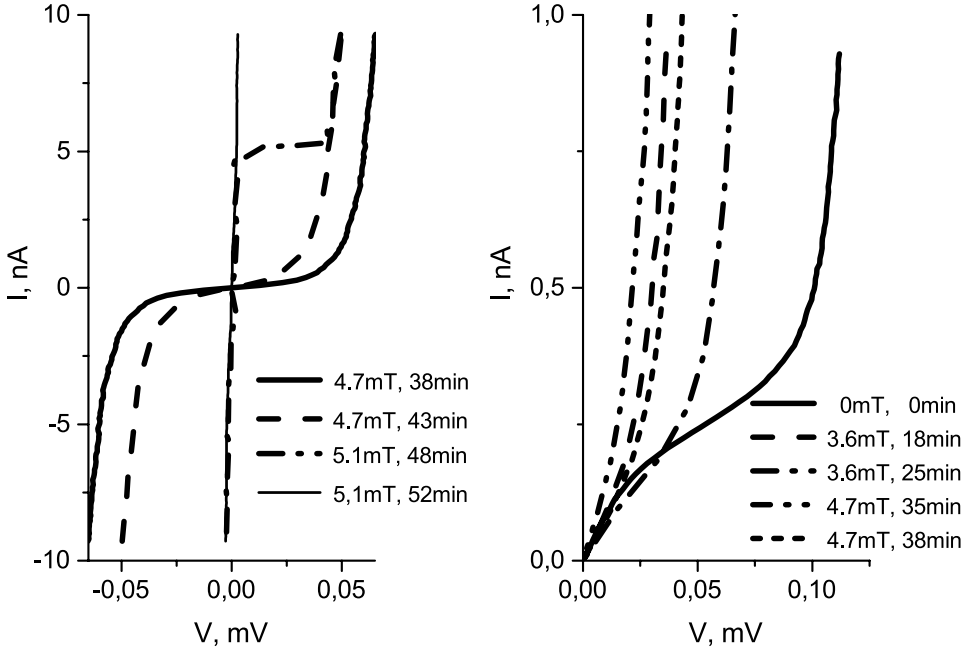

Fig. 5. I-V characteristics at different values of magnetic field normal to the surface of the SIN structure. The sequence of I-V characteristics recording is indicated in minutes from the start of recording the corresponding characteristic, the duration of recording each of them is approximately 2 minutes. During the recording of I-V characteristics at a field of 5.1 mT at 48 minutes, an abrupt transition occurred from an inhomogeneous field in the superconductor to the vortex state. Thus, $B_{c1} < 5$ mT. Note that the I-V characteristics measured at external field of 3.6 mT at 18 and 25 minutes and 4.7 mT at 35 and 38 minutes indicate the possibility of different configurations of inhomogeneous field in the superconductor with similar energy.

and allows to establish the influence of magnetic field on parameters of both subgap and single-electron currents.

3.1. Field Normal to the SIN Surface

Figure 5 shows I-V characteristics at different values of magnetic field normal to the surface of the SIN structure. The sequence of I-V characteristics recording is indicated in minutes from the start of recording the corresponding characteristic, with each recording taking approximately 2 minutes. During the I-V characteristic recording at 5.1 mT field at 48 minutes, a transition occurred from inhomogeneous field in the superconductor to the vortex state, as evidenced by a sharp change in differential conductance $G(V = 0, B = 0)$ from 1.15×10^{-5} Ohm^{-1} to 0.003 Ohm^{-1}. Apparently, this state does not correspond to the maximum vortex filling of the tunnel junction area, as in the experiment with cooling the sample from $T > T_c$ to 0.1K in a 4.7 mT field, the conductance at zero bias was 0.01 Ohm^{-1}. However, it remains significantly less than $1 / R_N = 0.032$ Ohm^{-1}. The vortex state is direct evidence that thin aluminum films are type-II superconductors [4, 5]. For the studied structure $B_{c1} < 5$ mT. Note that I-V characteristics measured at external field of 3.6 mT at 18 and 25 minutes and at 4.7 mT at 35 and 38 minutes demonstrate a "bounce back" as if to a lower field. This indicates the possibility of various configurations of inhomogeneous field in the superconductor with similar energy. These field distribution states are metastable with large hysteresis. Thus, the vortex structure remains unchanged when the field is turned off and is destroyed only in a field of opposite direction or when heated above T_c.

In pure aluminum $T << T_c$ critical field $B_c \simeq 11$ mT, coherence length $\xi_0 \simeq 1500$ nm, magnetic field penetration depth $\lambda_0 = 15$ nm. Fig. 6 shows the change in differential conductivity of the NIS structure in a magnetic field. It can be seen that at 14 mT, there is still a conductivity minimum due to aluminum superconductivity. This indicates that $B_{c2} / B_c > 1.3$. From the relation $B_{c2} B_{c1} = B_c^2$ at $B_{c1} = 5$ mT we have $B_{c2}/B_c \simeq 2.2$. Using the estimation $B_{c2} = \Phi_0 / 2\pi\xi^2$ (Φ_0 — magnetic flux quantum) we obtain that ξ lies in the interval 115–150 nm. From the relation $\xi^2 = \xi_0 l$ for the

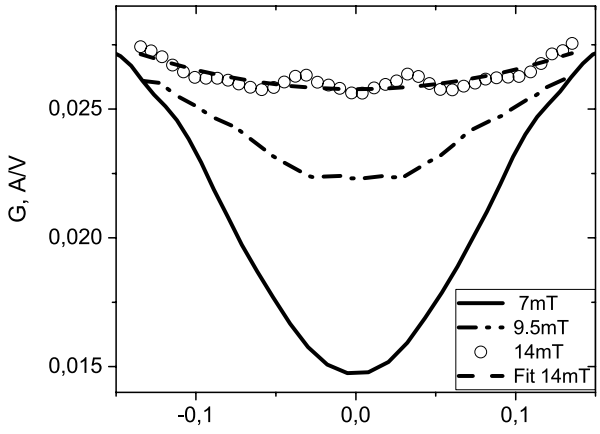

Fig. 6. Dependencies of differential conductivity of NIS1 on voltage at different magnetic field induction values perpendicular to the NS surface

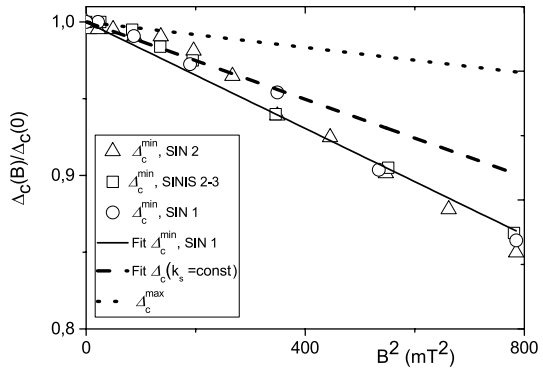

Fig. 7. Change in the superconducting gap in tangential magnetic field. $\Delta^{\min}$ — value determined from the field dependence of single-electron current component, $\Delta(k_s = \text{const})$ const) corresponds to constant value in formula (3) for Andreev current, $\Delta^{\max}$ corresponds to results of work [4] at $\xi = 150$ nm

electron mean free path in the aluminum film, we obtain $l = 9 - 15$ nm. And finally, for the penetration depth from the relation $B_{c1} / B_c = \lambda / l$ it follows that l lies in the interval 200–250 nm. Thus, the criterion for type-II superconductivity is met. (The relations used here are taken from [14, 15].)

Using the formula for the dependence of local conductivity of a quantum vortex on the distance from its center, obtained by tunnel spectroscopy in work [16],

$$G(x) = G_0 - \frac{G_N - G_0}{1 - \text{th}(x / \lambda)},$$

assuming the vortex is axially symmetric, we obtain for the conductivity of one vortex 0.0009 Ohm^{-1} (for $\lambda = 100$ nm) and 0.0019 Ohm^{-1} (for $\lambda = 150$ nm). With NIS conductivity in a field of 4.7mT equal 0.01 Ohm^{-1} m this corresponds to the inclusion of 11 or 5 vortices. The maximum number of vortices on the NIS area $S = 8$ μm^2 in a field of 4.7 mT in accordance with the relation $n = SB / \Phi_0 = 18$. According to work [17], for micron-sized samples such filling is not achieved due to penetration of the magnetic field at the film edges at dimensions of order l. Thus, for a circle with a diameter of 2 μm instead of 6, only vortices fit. Therefore, the NIS conductivity in fields greater than B_{c1}, agrees with the vortex structure pattern.

3.2. SIN in tangential field

3.2.1 Single-electron conductance

As shown in Fig. 1, the junction area has a complex geometry: it has a section with dimensions $2' 3$ μm^2, from which a strip $\simeq 1 \times 2$ μm^2 extends at right angle. These dimensions exceed the penetration depth. Therefore, in a magnetic field normal to the SIN surface, due to the Meissner–Ochsenfeld effect, its distribution is highly — practically absent in the middle, and at the junction edges exceeds the field at infinity by several times. As it turned out, in this case too, the measured I-V characteristics can be approximated by formulas (1)–(5). However, the results obtained in this case allow only qualitative conclusions. In the in-plane field, the situation is opposite — the thickness of the superconducting film 80 nm is significantly less than l. Using the corresponding formula for field distribution in a thin plate [15], one can estimate that the field in the middle of the film is 1–1.5% less than at infinity. This allows obtaining quantitative results.

According to Fig. 4, magnetic field leads to changes in single-particle current similar to temperature increase. But since constant field cannot heat SIN, the current increase means decrease in superconducting gap due to pair-breaking effect. Fig. 7 shows dependencies Δ_c for two SINs and for SINIS in tangential field. All three dependencies coincide within the error of this parameter determination.

These dependencies can be approximated by the formula

$$\Delta_c(B) / \Delta_c(0) = 1 - aB^2. \qquad (6)$$

According to [3], the gap changes as

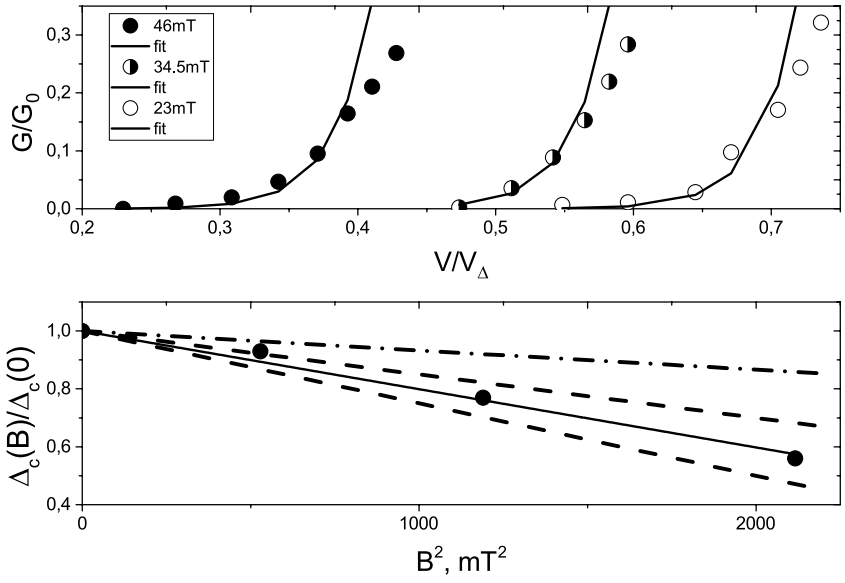

Fig. 8. Top: experimental points transferred from Fig. 3 of work [3], lines — fit using formula (1). Bottom: circles — values of $\Delta_c(B)/\Delta_c(0)$, solid line — linear function fit, dashed lines limit from below and above the area corresponding to the results shown in Fig. 7, taking into account possible scale changes in B^2 due to differences in parameters L × ξ in our work and in [3], dash-dot line – dependency $\Delta_c(B)/\Delta_c(0)$, established in [3] based on measurements in the voltage range near V_c

$$D_c(B) / D_c(0) = 1 - 0.75(B / B_G)^2. \quad (7)$$

In work [3], it is shown that the characteristic field B_G equals

$$B_G = \sqrt{6}he / dx = 0.78F_0 / (dx), \quad (8)$$

where F_0 is the magnetic flux quantum, and d and x are dimensions across the magnetic field direction (if $d < x$).By fitting the experimental values for SIN1 with expression (6), we get $B_G = 66$ mT. With a superconducting film thickness d =80 nm, according to (8), we get that the correlation length is $x = 340$ nm. However, as established in section 3.1, the value of x lies in the interval 115–150 nm. Note that at $x = 340$ nm aluminum is a type-I superconductor, which clearly contradicts experiments in a normal magnetic field.

Thus, the change in D_c of the superconductor, determined by the change in single-electron current under field influence, does not correspond to the model constructed in [3]. As noted above, in our case it was impossible to obtain sufficiently reliable information about the conductivity of the studied structures at $V \simeq V_c$. However, it can be shown that our experimental dependencies of differential conductivity on voltage "stitch together" with those presented in this publication. Thus, the dependencies $G(V)$ at $G(V) / G_n < 0.2$ shown in [3] can be fitted using formula (1), upper Fig. 8. The values of $D_c(B) / D_c(0)$ obtained this way are shown in the lower Fig. 8. To compare these data with our results (Fig. 7), we need to account for the magnetic field scale change. The values of $L * x$ in our work and in [3] are 0.014–0.018 and 0.015 μm^2 respectively

As can be seen, our data analysis results from work [3] at low conductance values are also located in this region. However, the values of $D_c(B) / D_c(0)$, corresponding to the conductance maximum near V_c, (dash-dotted line) demonstrate significantly less change in $D_c(B) / D_c(0)$ and correspond to the theory. Thus, there are two parameters that change quadratically with the field, characterizing the superconductor: D_c^{min}, which describes the exponential decrease in single-electron tunnel current with decreasing voltage, and D_c^{max}, which describes the conductance in the region of maximum conductance near V_c. In the absence of a field, they coincide. Accordingly, D_c^{min} has the meaning of a cutoff parameter in the Dynes spectrum, and, as a result, at low voltage values, there is a transition in describing the single-electron current from formula (5) to formula (1). The influence of the field, inclined to the surface or applied normally, can be described by formula (6), however, the coefficient at B^2 is larger by approximately two times and almost by 2 orders

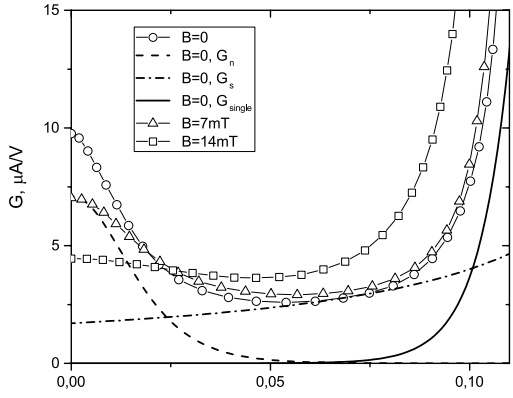

Fig. 9. Differential conductance at several values of tangential magnetic field induction and calculated conductance components in the absence of field

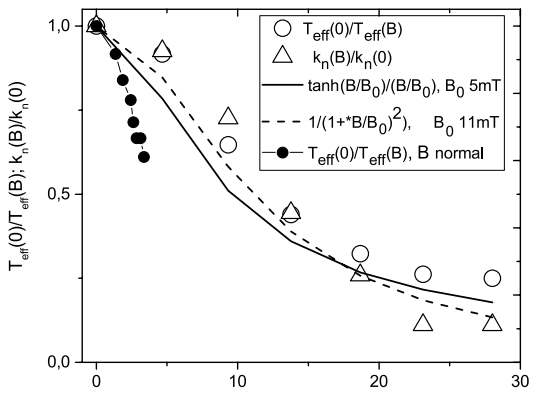

Fig. 10. Dependencies on tangential and normal to NIS surface magnetic field induction, normalized values of parameters k_n (at T_{eff} = const) and T_{eff} (at k_n = const), describing component I_n of Andreev current, formula (3) .

of magnitude. Qualitatively, this can be explained by the influence of two factors. First, in a normal field, instead of the size d one should use x, which will lead to an increase in coefficient*a* in formula (6) by 4.5 times. Second, while maintaining the total flux, the field in the central region of the film is small, but at the periphery, it significantly exceeds the field far from the superconductor. Therefore, practically all current is concentrated where the pair-breaking, proportional to the square of the field, is stronger. This more than compensates for the decrease in the effective junction area.

3.2.2 Andreev conductance, component I_n

Figure 9 shows the dependencies of differential conductance G SIN on voltage at several values of tangential magnetic field induction and current components obtained by fitting I-V characteristics at zero field according to formulas (1) and (3), Fig. 2. According to Fig. 9, the value dI_n / dV at voltage $V = 0$ corresponds to the value $G_A(V = 0) - G_{min}$, used in analyzing the effect of tangential magnetic field on Andreev conductance in work [6]. The authors of the cited work, referring to theoretical publications [18], used the formula

$$G_A(V = 0, B) =$$

$$= G_A(V = 0, B = 0)\text{th}(b) / b, \qquad (9)$$

$$b = 2^{1/2}\lambda LeB / \hbar = B / B_0,$$

where L is the length of the normal strip within which electrons diffuse. The value l is not given in [6]. According to this formula, the field affects k_n. The applicability of this approach raises questions. For aluminum film, as shown above and known from publications, l is 150–200 nm. Fig. 3 at field 0.28 T, an order of magnitude larger than in this article (Fig.9), at the same electron temperature 0.1 K, no single-electron current contribution is visible. Based on results from section 3.2.1, it can be stated that the film thickness is less than 80 nm by approximately 3 times or more. Using formula (9), one can estimate B_0 » 0.7 - 0.8 T, and with L =5 μm for the second dimension, about 1 nm remains. It seems the authors of [6] made a mistake in calculations, therefore one cannot accept that the theory is confirmed by experiment. Note also that it seems strange to use a parameter describing superconductor for describing processes in normal metal.

Figure 10 shows results of determining $k_n(B) / k_n(0)$ for SIN1 assuming that the value $T_{eff}(B = 0)$ =0.11 K is independent of field and $k_n(0)$ = 0.135nA in tangential magnetic field, and calculation of differential conductance at $V = 0$ using formula (9) with B_0 = 5 mT. If in formula (9) instead of l we substitute film thickness 20 nm, then for L we get value 5 μm, which is close to lateral dimensions of the normal film.

An alternative approach used in work [7] is based on qualitative arguments. In the formula for Andreev current I_n (2), the coefficient k_n does not

contain quantities dependent on magnetic field or temperature. And the temperature change leads to the fact that at $V = 0$ the differential conductivity, according to theory, changes proportionally to $1 / T_e$ (formulas (2) and (4)). In [7], it was established that in reality, instead of T_e one should use a slightly larger value T_{eff}, which is related to the presence of defects in the metal film. This is confirmed by the results obtained in [7] and presented below for a multi-element structure of series-connected SIN aluminum-aluminum oxide-aluminum with a thin iron sublayer suppressing superconductivity. In the latter case, T_{eff} exceeds the value of $T_e \simeq 0.1$ K several times. It is natural to assume that the magnetic field also leads to a change in effective temperature. Therefore, when fitting the I-V characteristics using formula (3), it was assumed that the magnetic field leads to a change in T_{eff}. Figure 10 shows the results of determining $1 / T_{eff}(B)$ at constant $k_n(0) = 0.135$ nA for SIN1 in a tangential magnetic field and calculation of differential conductivity at $V = 0$ using formula

$$T_{eff}(B) = T_{eff}(0)(1 + (B / B_0)^2) \qquad (10)$$

with $B_0 = \Phi_0 / (dl_\phi) = 11$ mT, where d is the film thickness of 20 nm, and $l_\phi \approx 9$ μm is the electron phase-breaking length. This formula is proposed by analogy with the description in work [19] of the proximity effect suppression in a mesoscopic film contacting a superconductor. The obtained value l_ϕ has a reasonable order of magnitude, especially considering that formula (10) was obtained from qualitative considerations. According to Figure 10, in both cases, agreement is achieved within the measurement error of dI_n / dV at $V = 0$. However, the next section shows that the model of effective temperature change under magnetic field influence can be preferred based on the change in $I_s(B)$ or $I_{Dynes}(B)$. Along with the results obtained in the tangential field, Figure 10 presents measurement results in the normal field. In this case, the Andreev conductivity changes more rapidly. The anomalous Andreev conductivity is suppressed by the field, and the central region, whose dimensions decrease with increasing field, begins to play the main role. However, such a local approach is hardly applicable since the lateral dimensions $L << l_\phi$. To make a correct comparison of the field effect on Andreev current at different orientations, experiments with structures whose width and thickness are comparable and significantly smaller than the penetration depth are needed to ensure field uniformity in the superconductor.

3.2.3 Andreev conductance, component I_s

According to formulas (2), (4), this current should depend on the magnetic field, primarily due to changes in $\Delta_c(B)$. The question arises which value should be taken or $\Delta_c^{min}(B)$, $\Delta_c^{max}(B)$ specific value describing the current $I_s(B)$ under condition $k_s = \text{const}$. As in the case of current $I_n(B)$, coefficient k_s in formulas (2), (4) does not contain field-dependent quantities. We are not aware of works discussing the field dependence of current I_s. Moreover, in most studies on SIN junctions, except for [7], this component of Andreev current is considered negligibly small, and instead, the Dynes current I_{Dynes} (5) is used when analyzing current-voltage characteristics. Figure 11 shows the results of determining these currents' parameters when fitting current-voltage characteristics using formulas (1), (3), (5) under the following assumptions.

1. When calculating current I_n we assume $k_n = \text{const}$, T_{eff} depends on field B.

1.1. k_s ((1), Fig. 11*a*), alternatively γ ((5), Fig. 11 *b*), change with field, gap $\Delta_c^{min}(B)$.

1.2. k_s ((2), Fig. 11*a*), alternatively γ ((6), Fig. 11*b*), change with field, gap $\Delta_c^{max}(B)$.

1.3. $k_s = \text{const}$ ((9), Fig. 11*c*) alternatively $\gamma = \text{const}$ ((10) Fig. 11*c*) gap values are selected during I-V curve fitting to satisfy this condition.

2. When calculating current I_n we assume $T_{eff} = \text{const}$, k_n depends on field B.

2.1. k_s (3), alternatively γ (7), change with field, gap $\Delta_c^{min}(B)$.

2.2. k_s (4), alternatively γ (points in Fig. 8), change with field, gap $\Delta_c^{max}(B)$.

2.3. $k_s = \text{const}$ (points in Fig. 11*c*) alternatively $\gamma = \text{const}$ (points in Fig. 12*c*) gap values are selected during I-V curve fitting to satisfy this condition.

In principle, a "hybrid" model is not excluded with selection of contribution ratio from changes in both k_n, and T_{eff}, ensuring constancy of k_s. However, with the current accuracy of current and voltage measurements, this is not meaningful.

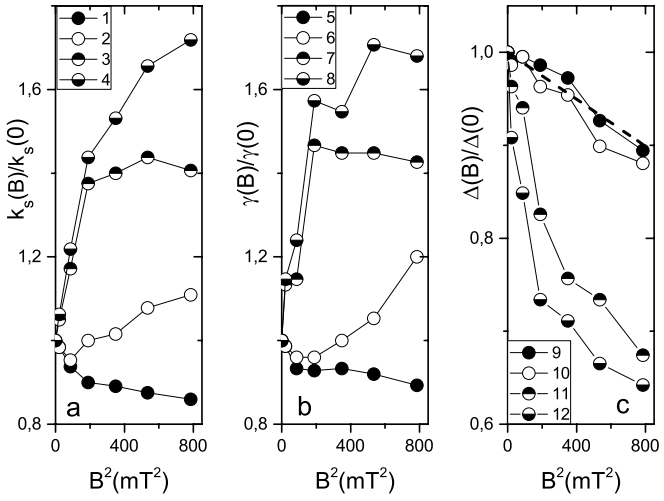

Fig. 11. Dependence of reduced coefficients on magnetic field induction applied in the SIN plane: *a* — k_s (Andreev current component); *b* — γ (Dynes current); with *c* — gap Δ(ks = const) and Δ(γ = const). Curves 1, 2, 5, 6, 9, 10 at k_n = const, 3, 4, 7, 8, 11, 12 at T_{eff} = const, curves 1, 3, 5, 7 at Δ^{min}, curves 2, 4, 6, 8 at Δmax

According to Fig. 11, all variants corresponding to point 2 and some variants of point 1 can be excluded from consideration. There are no grounds for increase with the Andreev current field I_s (dependencies 2, 3, 4). The Dynes current (dependencies) could, in principle, increase, but not by tens of percent, rather by several times due to significant broadening of the conductance peak in the maximum region near the gap [3]. The decrease in the superconducting gap, corresponding to the constancy T_{eff} and k_s (dependency 11) or g (dependency 12), significantly exceeds the change in D^{min}. Moreover, contrary to common sense, in all these cases and variants 1.2 (dependencies 1, 5), parameters rapidly change in the field region $B < 10$ mT, while with further field increase, the change slows down or even stops (dependencies 3, 7).

Thus, only 2 variants remain that correspond to an acceptable description of the pattern — k_n = const, T_{eff} depends on field B, D(k_s = const) (Fig. 11), dependency 9, alternatively D(g = const) (Fig. 11), dependency 10, and these gap values, like D^{min}, D^{max} decrease quadratically with field B (Fig. 7, 11).

4. CONDUCTANCE OF MULTI-ELEMENT STRUCTURE

In [4, 5, 7] the results of the normal-to-surface magnetic field influence and the contribution of Andreev current to the conductance of an "electron thermometer" — a structure containing 100 series-connected identical chains of 5 parallel-connected SINs are described. Each SIN contains an 80 nm thick aluminum electrode, aluminum oxide, and a normal electrode made of aluminum with an iron sublayer suppressing its superconductivity. The SIN junction area is 1.8 μm². Each junction is connected to adjacent gold films with dimensions 14×100×0.1 μm. With such structure configuration, thermal effects are suppressed.

Fig. 12 shows the current-voltage characteristic and the conductance obtained by its numerical differentiation of the thermometer and its fitting using formulas (1) and (3). The fitting curve using Dynes formula on the current graph is indistinguishable from the Andreev current fitting using formula (3). However, for conductance, there is a difference at small biases that significantly exceeds the measurement error. It is about a 8 % and appears because the measured voltage is a hundred times larger than for a single SIN junction, and therefore the signal-to-noise ratio is significantly higher.

Note that the anomaly in differential conductance — the maximum at $V = 0$, due to Andreev current I_n, is not visible. This is because $T_{eff} = 1 \pm 0.3$ K. Obviously, this is related to the magnetic moment of iron atoms, which supports the model of magnetic field influence on effective temperature.

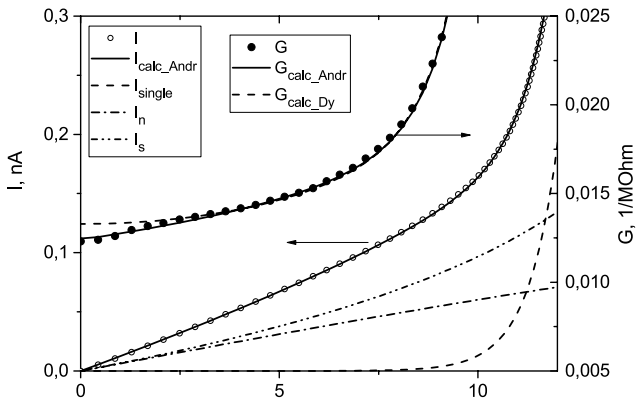

Fig. 12. Measured I-V characteristics and differential conductance of the electronic "thermometer" consisting of 100 series-connected NIS junctions and their fitting using formulas (1), (3), (5). Fitting parameters: $R_n/100 = 90$ Ohm; $\Delta c/k = 2.07$ K; $T_e = 0.087$ K. For Andreev current $I_{Andreev}$; $T_{eff} = 1$ K; $k_n = 0.098$ nA; $k_s = 0.12$ nA. For Dynes current: $T_e = 0.0865$ K; $T_{eff} = 1$ K; kn = 0.022 nA; $\gamma/\Delta c = 1.07 \cdot 10^{-4}$

5. DISCUSSION OF RESULTS

The study of conductance in thin-film SIN structures in a magnetic field normal to their surface allowed to estimate the parameters of the superconducting film — correlation length x and field penetration depth l . Thanks to this, it was possible to identify the peculiarity of the magnetic field influence, oriented in the structure plane with thickness much less than the penetration depth, on its conductance. At low voltage across the structure, when its resistance at low temperature is much higher than R_n, the single-electron current, as in the absence of field, is described by formula (1). However, the value of Δ_c appearing in it changes with field much faster than follows from theoretical consideration of pair-breaking and experiments in work [3]. Such behavior can be interpreted as cutting of the Dynes spectrum and transition from formula (5) to exponential current decay with decreasing voltage.

The two-particle Andreev current (3) is determined as the difference between the measured current and the calculated single-electron current. In the field, the change of component I_n is described by the change in effective temperature T_{eff} at a constant coefficient value k_n. The change in I_s can be described if we assume that k_s is field-independent, while D changes quadratically with the field.

Although there is no place for the Dynes current used in most studies of SIN structures in this picture, in the present work such a model was considered as an alternative to the Andreev current I_s. In almost all cases, except for the multi-element "electronic thermometer," within measurement uncertainty, it was possible to fit the measured current-voltage characteristics within both models with similar results concerning the changes in SIN parameters in the magnetic field. However, due to high measurement accuracy for the multi-element structure, a linear increase in conductivity at low voltages was revealed (Fig. 12), which is characteristic of the Andreev current described by formulas (2), (3) and contradicts the conductivity determined by the Dynes current (5).

The Dynes current is due to an imaginary addition in the excitation spectrum in the superconductor associated with their scattering. This leads to broadening of the maximum at $V \simeq \Delta_c/e$. It is natural to expect that a significant, several-fold broadening of this peak in the magnetic field [3] should increase the Dynes current by the same amount. But this does not occur. Finally, in work [6] for structures manufactured using the same technology, differing only in the thickness of the insulating layer, it turned out that in the Dynes model, the parameter g, which depends only on the parameters of the superconducting film, changes by an order of magnitude. At the same time, as seen in Fig. 3 of this work, the ratio of Andreev conductance due to current I_n, to the additional subgap conductance remains practically constant, which is natural for Andreev current components. Note that in [7], for different samples, the ratio of these contributions also changes very moderately — no more than threefold.

The main reason why current I_s is ignored is that according to the theoretical formula (2), the ratio I_s, is ignored is that according to the theoretical formula (2), the ratio $k_s / k_n << 1$. And according to experiment [7], for different structures, it lies within 2 – 7, tens of times larger than predicted by theory. However, if formula (4) is used for estimation, the discrepancy with the experiment decreases approximately threefold. According to measurements in [6, (Fig.4)], for films with thickness $d > l$ instead of d in the corresponding formulas, the mean free path l.should be used. For a superconducting film with d =80 nm and mean free path l = 9–15 nm

(section 3.1), this will lead to an increase in the calculated value of k_s by 5–9 times. The copper film has d =20 nm and l » 10 nm [7], so k_n will change insignificantly. Taking this circumstance into account makes the difference between theory and experiment less dramatic.

Thus, to describe the conductivity of tunnel SIN structures both in magnetic field and without it, at temperatures much lower than T_c, and at voltages where the tunnel current is much lower than the current in the normal state of the superconducting film, three components are sufficient: single-electron current, formula (1), and two components of Andreev current, formula (3). Meanwhile, regardless of the magnetic field orientation relative to the structure plane, the single-electron current contribution grows proportionally to the square of the field due to its effect on the superconducting gap. The conductivity due to Andreev current I_n, decreases due to the increase in effective temperature. The change in current I_s can be described by gap reduction. We are not aware of works that consider the magnetic field's influence on this component of tunnel current.

To make these conclusions even more substantiated, it would be advisable to conduct experiments with similar SIN structures having a thinner superconducting layer and width less than the penetration depth. This will allow, by reducing the magnetic field's influence on single-electron current, to expand the voltage range where the subgap current dominates and to conduct measurements with orthogonal field orientation while maintaining field uniformity within the structure.

ACKNOWLEDGMENTS

The authors are grateful to Alexander Fedorovich Andreev for his interest in the work and useful discussions. The equipment of the Unique Scientific Installation No. 352529 “Cryointegral” was used in performing the work.

FUNDING

This work was supported by the Russian Science Foundation, grant https://rscf.ru/project/23-79-00022/.

REFERENCES

1. J. L. Levine, Phys. Rev. v. 155, p. 373 (1967)
2. J. Millstein, M. Tinkham, Phys. Rev. v.158, p. 325 (1967)
3. A. Anthore, H. Pothier, and D. Esteve, Phys. Rev. Lett. 90, 127001 (2003)
4. M.A. Tarasov, V. S. Edelman, JETP Letters, v.101, p. 740 (2015)
5. Mikhail Tarasov, Aleksandra Gunbina, Mikhail Fominsky, Artem Chekushkin, Vyacheslav Vdovin, Valery Koshelets, Elizaveta Sohina, Alexei Kalaboukhov and Valerian Edelman, Electronics 2021, 10, 2894. https://doi.org/10.3390/electronics10232894
6. Tine Greibe, Markku P.V. Stenberg, C. M. Wilson, Thilo Bauch, Vitaly S. Shumeiko, and Per Delsing. PRL 106, 097001 (2011)
7. A. V. Seliverstov, M. A. Tarasov, V. S. Edelman, JETP, v. 124, p. 643 (2017)
8. Giaever, I., Megerle, K., Phys. Rev., v. 122, p. 1101 (1961)
9. F. W. J. Hekking and Y. V. Nazarov, Phys. Rev B., vol. 49, p. 6847, (1994)
10. T. Faivre, D. S. Golubev, J. P. Pekola, Appl. Phys. Lett. 106, 182602 (2015)
11. R. C. Dynes, V. Narayanamurti, J. P. Garno, PRL, vol. 41, No.21, p. 1509 (1978)
12. A. V. Feshchenko, L. Casparis, I. M. Khaymovich, D. Maradan, O.-P. Saira, M. Palma, M. Meschke, J. P. Pekola, and D. M. Zumbühl, Phys. Rev. Applied 4, 034001 (2015)
13. V. S. Edelman, IET, v.52,p.301 (2009)V
14. Charles Kittel, Introduction to solid state Physics, 4 edition, John Willey&Sons, Inc
15. V. V. Shmidt, Introduction to the Physics of Superconductivity, (2000).
16. M. R. Eskildsen, M. Kugler, G. Levy, S. Tanaka, J. Jun, S. M. Kazakov, J. Karpinski, Ø. Fischer, Physica C: Superconductivity, v. 385, Issues 1-2, p. 169 (2003)
17. I. V. Grigorieva, W. Escoffier, J. Richardson, L. Y. Vinnikov, S. Dubonos, and V. Oboznov, Phys. Rev. Lett. 96, 077005 (2006)
18. A. F. Volkov and T. M. Klapwijk, Phys. Lett. A 168, 217 (1992); A. F. Volkov, Phys. Lett. A 174, 144 (1993); A.F. Volkov, A.V. Zaitsev, and T. M. Klapwijk, Physica (Amsterdam) 210C, 21 (1993); A. F. Volkov, Physica (Amsterdam) 203B, 267 (1994).
19. D. A. Dikin, M. J. Black and V. Chandrasekhar, Phys. Rev. Lett. 87, 187003 (2001) DOI:https://doi.org/10.1103/PhysRevLett.87.187003